Modeling macroroughness contribution to fish habitat-suitability curves

Water Resources Research

RESEARCH ARTICLE
10.1029/2018WR022860

Modeling Macroroughness Contribution to Fish Habitat Suitability Curves

Amin Niayifar[1], Holly J. Oldroyd[2], Stuart N. Lane[3], and Paolo Perona[4]

[1]Stream Biofilm and Ecosystem Research Laboratory, Institute of Environmental Engineering, EPFL-ENAC, Lausanne, Switzerland, [2]Department of Civil and Environmental Engineering, University of California, Davis, CA, USA, [3]Institute of Earth Surface Dynamics, University of Lausanne, Lausanne, Switzerland, [4]School of Engineering, Institute for Infrastructure and Environment, The University of Edinburgh, Edinburgh, UK

Key Points:
- We develop an analytical approach to model the usable habitat area generated by stones in alpine streams
- Stone size distribution strongly affects the subsequent threshold flows and the associated ecological impacts
- This model combined with multiobjective optimization analysis can be used to determine physically based flow release policies

Correspondence to:
A. Niayifar,
a.niayifar@gmail.com

Citation:
Niayifar, A., Oldroyd, H. J., Lane, S. N., & Perona, P. (2018). Modeling macroroughness contribution to fish habitat suitability curves. *Water Resources Research*, *54*, 9306–9320. https://doi.org/10.1029/2018WR022860

Received 1 MAR 2018
Accepted 27 OCT 2018
Accepted article online 5 NOV 2018
Published online 23 NOV 2018

Abstract Improved water management strategies necessitate a solid understanding of environmental impacts associated with various flow release policies. Habitat suitability models use hydrodynamic simulations to generate weighted usable area curves, which are useful in characterizing the ecological suitability of flow release rules. However, these models are not conveniently run to resolve the hydrodynamics at the smaller scales associated with macroroughness elements (e.g., individual stones), which produce wakes that contribute significantly to habitat suitability by serving as shelter zones where fishes can rest and feed. In this study, we propose a robust environmental indicator that considers the habitat generated by the wakes downstream of stones and can thus be used to assess the environmental efficiency of flow release rules for impounded streams. We develop an analytical solution to approximate the wake areas behind macroroughness elements, and the statistical distribution of wake areas is then found using the derived distribution approach. To illustrate the concept, we apply our theory to four exemplary river streams with dispersed stones having different statistical diameter size distributions, some of which allow for an analytical expression of the weighted usable area. We additionally investigate the impact of spatiotemporal changes in stone size distributions on the usable area and the consequent threshold flows. Finally, we include the proposed environmental indicator to solve a multiobjective reservoir optimization problem. This exemplifies its practical use and allows stakeholders to find the most favorable operational rules depending on the macroroughness characteristics of the impounded stream.

1. Introduction

Changing the natural flow regime causes an environmental degradation in alpine streams. Such changes occur due to climate change and other anthropic pressures (e.g., hydropower, irrigation, and urban and industrial uses) on alpine streams (Arthington et al., 2006; Assani et al., 2010; Birsan et al., 2005; Poff et al., 1997). Quantifying the environmental impacts of altering the natural flow regime on the riverine ecosystem still remains difficult and hence, controversial. Environmental indicators are typically used to assess the extent of disturbances in a riverine ecosystem, and indicators based on the habitat availability have been widely used in the literature (e.g., Bloesch et al., 2005; Razurel et al., 2016). Habitat availability is often assessed for different species by using modeling software such as CASiMir and PHABSIM (Maddock, 1999; Milhous et al., 1989; Schneider, 2001). These software packages model weighted usable area (WUA) curves for the fishes to define a fixed threshold for minimal flow releases, or the rules imposed, usually by government entities, to continually release at least a minimum discharge to the environment. Determination of this minimum is typically based on the break point of the WUA curve or the point below which the habitat suitability for the fishes decreases significantly. There are different approaches proposed to define break points (e.g., Annear & Conder, 1984; Gippel & Stewardson, 1998; Stalnaker & Arnette, 1976), and a common technique used in habitat suitability modeling is to consider the break point to be the discharge for which the WUA curve is maximized. The fish habitat indicator is then calculated by counting the maximum number of consecutive days characterized by flows below this critical threshold (e.g., Capra et al., 1995; Razurel et al., 2016).

The WUA curve and the associated threshold are calculated based on the streamflow characteristics such as the flow velocity. The threshold is very sensitive to the low velocity regions, that is, quiet zones at the bank, in

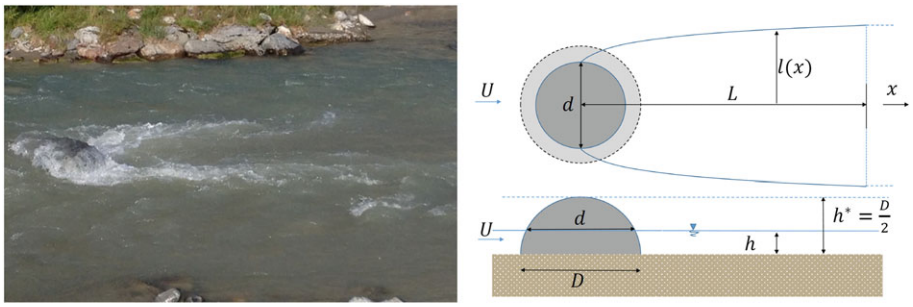

(a) (b)

Figure 1. (a) A visual example of the macroroughness effects on local river flow (b) schematic of the wake and related variables.

wakes behind macroroughness elements (i.e., big stones), etc. (Carolli et al., 2017). Figure 1a shows an exemplary change in the flow pattern due to the presence of a macroroughness element, marked by a significant decrease in flow velocity in the wake region. These low velocity or stationary regions act as refuge zones, as fishes minimize energy expenditure by resting in such regions where they can also quickly move to nearby faster waters to feed (Hayes & Jowett, 1994). Some recent studies have investigated the role of swimming energetics in fish habitat suitability (e.g., Enders & Boisclair, 2016; Lacey et al., 2012; Taguchi & Liao, 2011; Tritico & Cotel, 2010). For example, Enders et al. (2005) proposed a relationship to calculate the swimming cost for juvenile Atlantic salmon (salmo salar) based on the local hydrodynamic conditions and the fish body mass. Position choice and swimming costs of salmo salar in turbulent flow was also studied by Wilkes et al. (2017) who found that fishes most often select the cells adjacent to obstacles (i.e., in wakes). Additionally, these low shear stress zones significantly affect the diversity of periphyton and invertebrates in a stream (Biggs et al., 1997). Furthermore, the enhancement of the local turbulence intensity near the edges of the wakes results in an increased oxygenation rate (Moog & Jirka, 1999). In general, all of these factors make wake regions suitable fish habitats.

Numerical software packages can model the usable area curves corresponding to the riverine ecosystem on large scales, but their low spatial resolution is not able to capture the smaller-scale features such as the wakes downstream of macroroughnesses (i.e., big stones). Substantial advancements in computer science and technology have made it possible to develop high-resolution 2-D models (e.g., Ernst et al., 2010; Pasternack et al., 2008). These models can have up to meter resolution and therefore, in the future, might also be able to efficiently resolve the wakes associated with very large boulders over long river reaches. However, for a full river-scale simulation, the typical mesh resolution scale used in 2-D numerical simulations is larger than the macroroughness size for practical reasons (Lane et al., 2006) and also to reduce computational costs in 3-D models. Consequently, the presence of macroroughness elements is filtered (or cannot be properly resolved), and their effects on the simulated WUA curves are omitted. Habitat suitability models, at best, can consider a criterion of presence/absence of stones at the mesoscale as an input to determine the suitability of a mesohabitat (Parasiewicz, 2007; Vezza et al., 2014). However, these approaches are rather qualitative and do not directly calculate the wake areas associated with stones of various size distributions.

There have been extensive numerical and experimental studies investigating the effects of obstacles on the free stream flow (e.g., Coutanceau & Bouard, 1977; Roulund et al., 2005; Tennekes & Lumley, 1972). Complex flow patterns generated by a single macroroughness element and the associated ecological impacts have been further investigated by using computational fluid dynamic models (Shen & Diplas, 2008). Negretti et al. (2006) developed an analytical solution for the characteristic spatial scales of a turbulent wake in shallow flows. They started from the depth-averaged mass conservation equation and Reynolds-averaged equations for shallows flows and found an approximated solution by introducing scaling arguments and using the dominant balance approach, which considers only leading-order terms. Their solution consists of two analytical expressions to characterize the longitudinal and transversal length scales of shallow flow wakes.

Flow around rocks and the consequent ecological ramifications have also been studied in laboratory experiments and field studies. For example, Moghadam and Keshavarzi (2007) measured the flow structure behind a quarter-sphere fish habitat, mimicking a stone, in a laboratory flume. They characterized the low velocity

wake region downstream of the *stone* that is favorable for fishes for various flow depths. In addition to ecologically favorable wake velocities, lab experiments have shown that macroroughness elements play a role in enhancing the oxygenation rates in streams (e.g., Kucukali & Cokgor, 2008), which promotes overall ecological health and helps to sustain habitat for aquatic life (Kramer, 1987). These enhanced oxygenation rates have been found to sharply decrease as the macroroughnesses start to become submerged due to the decrease of the free surface turbulence level. Furthermore, field studies by Buffington et al. (2004) in mountain catchments indicate that hydraulic roughnesses are important fish spawning habitats.

In this paper, we aim to develop an analytical approach to model the total wake area for alpine water courses characterized by the presence of sparsely distributed macroroughness elements, that is, stones, whose spatial characteristics could be obtained via remote sensing techniques (e.g., drones and image processing). To investigate the model's capabilities and exemplify its practical use, the model is applied to four examples of stones with sparse but different statistical distributions of diameter sizes. We use these to calculate the respective usable area curves as a function of discharge, which can be used to define environmental flow thresholds for alpine streams. We further investigate the impact of stone size distributions on the threshold flow and apply the results in a multiobjective optimization problem to find the most efficient operational release rules for a hydropower system. This paper is structured as follows: The analytical model is described in section 2, followed by results presented in section 3. Finally, a discussion of the model results and conclusions are provided in sections 4 and 5, respectively.

2. The Model

2.1. Usable Area Behind a Single Stone

We consider a straight river reach of width, w, slope, s, and bed roughness given by an average Manning coefficient, n, which includes the resistance to the bulk flow introduced by the presence of macroscale roughness elements. We assume local, uniform flow conditions for the flow rate, Q, which can, however, slowly change in time, and stones are considered to be hemispherically shaped with maximum diameter, D. The range of hydrodynamical conditions suitable for fish habitat can vary by species. However, favorable habitat conditions generally tend toward lower velocities, and so we additionally assume that the low velocity wake region is usable habitat area (e.g., Buffington et al., 2004; Kucukali & Cokgor, 2008), as detailed in section 1.

From the Manning-Strickler relationship, we obtain the river depth, h

$$h = \left(\frac{Qn}{ws^{1/2}}\right)^{3/5}, \tag{1}$$

which also determines whether a stone is partially submerged ($h < \frac{D}{2}$) or fully submerged ($h \geq \frac{D}{2}$), as shown in Figure 1b. Note that $h^* = \frac{D}{2}$ denotes the water depth where the stone becomes submerged. In this case, we assume the wake is no longer relevant for defining *suitable* conditions. This assumption is validated by study by Moghadam and Keshavarzi (2007), which shows a significant reduction in the wake size when the *stone* becomes submerged. In addition, a submerged stone does not perturb the free surface to enhance oxygen entrainment and therefore cannot benefit the stream by increasing the oxygenation rate (Kucukali & Cokgor, 2008). From equation (1), the submerged condition can be specified in terms of the flow rate, Q_D, submerging stones of size, D, that is,

$$Q_D = \frac{D^{5/3}s^{1/2}w}{2^{5/3}n}. \tag{2}$$

For the partially submerged condition with a given flow rate, Q, the water surface intersects the stone of size D at the elevation, h, where the local, free surface stone diameter, d, is

$$d = \frac{2h}{\tan[\arcsin[\frac{2h}{D}]]} = D\sqrt{1 - \frac{4\left(\frac{nQ}{\sqrt{s}w}\right)^{6/5}}{D^2}}, \tag{3}$$

which is a function of both D and Q (see also Figure 1b).

Under the assumption that the stone's wake is determined by its diameter at the water surface (for given submergence conditions), we use the analytical model of Negretti et al. (2006) to estimate the longitudinal and

transversal expanse of the wake in the far wake region. It should be mentioned that the analytically derived wake size for a cylinder, as used by Negretti et al. (2006), provides a slightly conservative estimate of the wake region for a hemisphere that has a larger diameter at lower depths. For shallow water flow, Negretti et al. (2006) derived the longitudinal interaction length, L, from first principles, which reads

$$L = \frac{8h}{f_d}, \tag{4}$$

where f_d is the river bed friction factor, which is related to the Manning coefficient by

$$f_d = \frac{8n^2 g}{h^{1/3}}, \tag{5}$$

where g is gravitational acceleration. They additionally derived the transversal width of the wake as

$$l = d\sqrt{\frac{1 - e^{-\frac{x}{L}}}{8S}}, \tag{6}$$

where e is the exponential function, x is the distance downstream from the stone center, and S is the stability number, which is defined as (Negretti et al., 2006)

$$S = \frac{f_d}{4}\frac{d}{h}. \tag{7}$$

Note that L equation (4) depends on the hydrodynamic conditions, whereas equation (6) also depends on the stone size and varies as a function of L (see also Figure 1b). Hence, for a given stone size and set of hydrodynamic conditions, we can develop an expression for the area of the wake behind a stone. Since $L >> D/2$, the wake area is much larger than half of the horizontal cross-sectional area of the stone. In addition, we assume that the far-wake solution by Negretti et al. (2006) also provides a reasonable estimate of the near-wake areal expanse. Therefore, we obtain the wake area, A_w, by integrating the analytical expression for l, the transversal length scale equation (6), from the stone center to the longitudinal interaction length, L,

$$A_w = 2\int_0^L l(x)\mathrm{d}x = 2L\left(\mathrm{d}\frac{h}{2f_d}\right)^{1/2} B, \tag{8}$$

where B is a constant given by equation (10). Finally, combining equation (8) with equations (1), (4), and (5), one finds

$$A_w = \sqrt{\frac{D\sqrt{1 - \frac{4\left(\frac{nQ}{\sqrt{sw}}\right)^{6/5}}{D^2}}\left(\frac{nQ}{\sqrt{sw}}\right)^{12/5}}{4g^3 n^6}}B, \tag{9}$$

where

$$B = -2C + \ln\left(\frac{1+C}{1-C}\right) \tag{10}$$

and

$$C = (1 - \frac{1}{e})^{1/2}. \tag{11}$$

Hence, for a given stone size, D, the wake area given by equation (9) is the available habitat, or usable area, behind a single stone as a function of the flow rate, Q, stream width, w, slope, s, and Manning coefficient, n. Figure 2 shows the usable area as a function of specific flow rate, $Q^* = \frac{Q}{\sqrt{sw}}$, for different stone diameters and Manning coefficients. This area increases nonmonotonically for increasing flow rate, Q; that is, it increases up to a maximum, $A_w^{\max}$ and then decreases to 0 in correspondence with the flow rate, Q_D, for which the stone becomes submerged, that is, equation (2).

Thus, the wake size is flow limited for flow rates approaching 0 and becomes obstacle-size limited for flow rates approaching Q_D. Alpine streams may not dry up completely and the flow-limited condition may not be

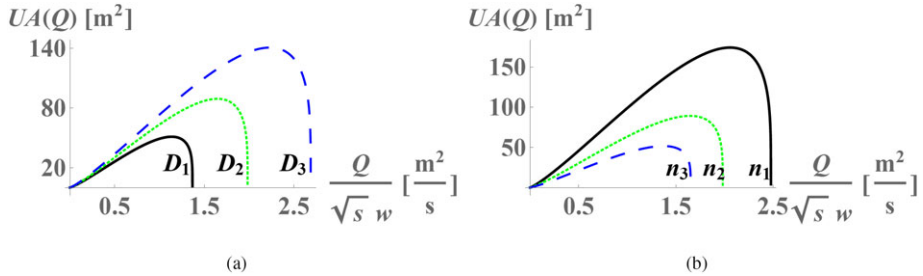

Figure 2. Exemplary visualization of the wake area with different parameters: (a) different stone diameters (n=0.05 $[\frac{s}{m^{1/3}}]$); $D_1 < D_2 < D_3$(b) different Manning coefficients (D=0.5 [m]); $n_1 < n_2 < n_3$. UA = usable area.

reached. We will, however, include the possibility that the water course dries up for the sake of generality. To upscale this result for usable area (UA), we additionally calculate the total wake area for stones randomly and sparsely distributed in a river reach and investigate how it changes for varying flow conditions.

2.2. Total Usable Area Behind Randomly Distributed, Sparse Stones

As in Figure 1, stones can be assumed to be sparse and distributed randomly in the river reach. If no two wakes interact, that is, that each wake is dependent only on D and the *bulk* hydrodynamic conditions, then the relative distance between any two stones is larger than L, the interaction length equation (4), for any flow rate, $0 < Q < Q_{D_{max}}$, where $Q_{D_{max}}$ is the flow rate for which the largest stone in the size distribution becomes submerged. Stones are detectable from aerial view, and assuming they are approximately semi-spherical, the characteristic size density distribution, $p_s(D)$, can be determined (e.g., by surveying with a drone and implementing image processing; see section 4.2).

Note that for a given, specific flow rate, Q^*, equation (9) also provides the change in total wake area for variable stone size (Figure 3). Supposing stones are distributed sparsely and with a size density distribution, $p_s(D)$, defined in the range $(D_1 \le D \le D_2)$ such that $\int_{D_1}^{D_2} p_s(D)\mathrm{d}D = 1$, where D is the dummy variable of integration, the density distribution of the wakes for a given flow rate can be obtained by using the derived distribution approach. First, we invert the wake-stone size relationship equation (9) to obtain

$$D(A_w) = \frac{2\sqrt{\frac{\left(\frac{nQ}{\sqrt{s}w}\right)^{6/5}(B^4Q^6+4A_w^4g^6n^6s^3w^6)}{B^4Q}}}{Q^{5/2}}, \tag{12}$$

through which the conditional density function of the wakes given Q, $p_w(A_w|Q)$ is

$$p_w(A_w|Q) = p_s(D(A_w))\left\|\frac{\mathrm{d}D}{\mathrm{d}A_w}\right\|, \tag{13}$$

where

$$\frac{\mathrm{d}D}{\mathrm{d}A_w} = \frac{16A_w^3g^6n^6s^3\left(\frac{nQ}{\sqrt{s}w}\right)^{6/5}w^6}{Q^{7/2}B^2\sqrt{\frac{\left(\frac{nQ}{\sqrt{s}w}\right)^{6/5}(4A_w^4g^6n^6s^3w^6+B^4Q^6)}{Q}}}. \tag{14}$$

This conditional density distribution function is defined within the range $(A_{w1}(Q) \le A_w \le A_{w2}(Q))$, where the limits, $A_{w1}(Q)$ and $A_{w2}(Q)$ are given respectively by

$$A_{w1}(Q) = \begin{cases} A_w(D_1) & Q \le Q_{D_1}, \\ 0 & Q > Q_{D_1}, \end{cases} \tag{15}$$

and

$$A_{w2}(Q) = \begin{cases} A_w(D_2) & Q \le Q_{D_2}, \\ 0 & Q > Q_{D_2}. \end{cases} \tag{16}$$

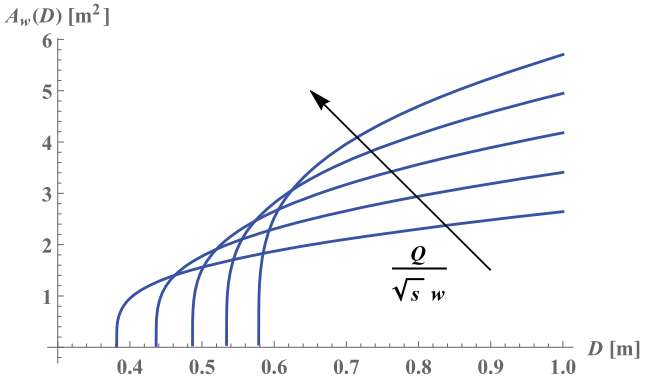

Figure 3. Wake area as a function of stone size using different parameters ($n = 0.05[\frac{s}{m^{1/3}}]$). Notice that all stones with a size smaller than D_m are submerged and do not contribute.

It should be noted that in equations (15) and (16), Q is included as a varying parameter, which enhances the boundaries for A_w.

Therefore, the normalized usable area, $UA_n(Q)$, provided by the stones for a given flow rate is the weighted sum of the individual wake areas,

$$UA_n(Q) = \int_{A_{w1}(Q)}^{A_{w2}(Q)} \omega_w p_w(\omega_w, Q) d\omega_w, \tag{17}$$

where ω_w is the dummy variable of integration. The fraction of submersed stones for a given flow rate that do not contribute is simply an atom of finite probability at 0 for $p_w(A_w)$,

$$p_w^{at}(0) = \int_{D_1}^{D_m} p_s(\delta) \mathrm{d}\delta, \tag{18}$$

where δ is the dummy variable of integration and D_m is the diameter in which all the stones get submerged. Equation (17) can be plotted for varying flow rate conditions to build up the normalized usable area as a function of the flow rate and $D_1 \leq D \leq D_m$ as the range of stones already submerged. Hence, by using known (or surveyed) frequency distributions for each stone size, the normalized usable area, UA_n from equation (17), returns the sum of the real usable area associated with each stone size for a given flow rate.

2.3. Threshold Flow

Once the usable area curve is found, it can be used to help define the environmental threshold for managing stream discharge. We define this threshold as the flow rate for which the usable area is maximal, which implies that the derivative of the usable area curve becomes 0. Flow rates lower than this threshold (Q_t) are critical for the riverine ecosystem as the ecological benefits associated with the wake area generated by macroroughness elements rapidly decreases. The following is the mathematical definition of the environmental threshold:

$$\frac{\mathrm{d}UA}{\mathrm{d}Q} \Big|_{Q_t} = 0. \tag{19}$$

3. Results

3.1. The Impact of Stone Size Distributions on the Usable Area Curve

3.1.1. Stone Size Distributions

We investigate the model's behavior by showing some examples using different stone size distributions. The range of stone sizes, number of stones, and stream parameters used in the test cases are given in Table 1. For these examples, we maintain the assumptions that the spatial distributions are sparse and stones are hemispherically shaped, as discussed above.

Example 1: Stones with a constant diameter size distribution. This example utilizes a Dirac delta function (Figure 4a) to prescribe the size distribution of stones with diameters, $D = D^*$, that is,

$$p_s(D) = \delta(D - D^*), \tag{20}$$

where

$$\int_0^\infty p_s(D) \mathrm{d}D = 1. \tag{21}$$

As the Dirac delta distribution is discontinuous, the distribution of the wakes will also be a Dirac delta function around the wake area, A_w^*, as given by equation (9) for $D = D^*$,

Table 1
Stone and Stream Parameters Used in Examples Cases

Range of stones diameter [m]	Number of stones	Manning's coefficient	Width [m]	Slope
$0.1 < D < 0.7$	$N = 50$	$n = 0.05[\frac{s}{m^{1/3}}]$	$w = 5$	$s = 0.01$

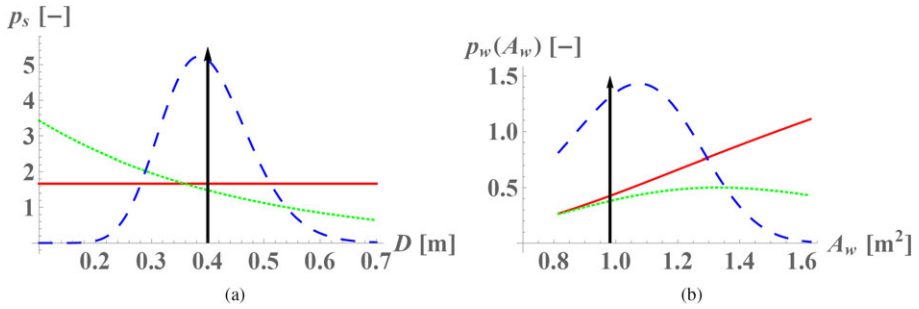

Figure 4. Statistical distribution of (a) stones diameters $0.1 < D < 0.7$ m (number of stones; $N = 50$) and (b) wake area for an assigned flow rate. The thick black arrow denotes the delta distribution, the red curve shows the uniform distribution, and the green dotted and blue dashed curves represent the truncated exponential and truncated gamma distributions, respectively. The probability density functions of the wake area correspond to the flow rate $Q = 0.5[\frac{m^3}{s}]$.

$$p_w(A_w|Q) = \delta(A_w - A_w^*), \tag{22}$$

whose integral over the wake sizes gives the cumulative distribution,

$$P_w(A_w|Q) = \int_0^\infty \delta(\omega_w - \omega_w^*)d\omega_w = \Theta\left(\sqrt{\frac{D^*Q^2\sqrt{1-\frac{4\left(\frac{nQ}{\sqrt{sw}}\right)^{6/5}}{D^{*2}}}\left(\frac{nQ}{\sqrt{sw}}\right)^{2/5}}{g^3n^4sw^2}}\right), \tag{23}$$

where ω_w is the dummy variable of integration and $\Theta(\cdot)$ is the Heaviside function. Note that the Heaviside function depends on the flow rate, Q, because the location of the Dirac delta distribution for A_w is a function of Q. For this case, the usable area becomes

$$UA(Q) = N\sqrt{\frac{D^*\sqrt{1-\frac{4\left(\frac{nQ}{\sqrt{sw}}\right)^{6/5}}{D^{*2}}}\left(\frac{nQ}{\sqrt{sw}}\right)^{12/5}}{4g^3n^6}}\Theta\left(\sqrt{\frac{D^*Q^2\sqrt{1-\frac{4\left(\frac{nQ}{\sqrt{sw}}\right)^{6/5}}{D^{*2}}}\left(\frac{nQ}{\sqrt{sw}}\right)^{2/5}}{g^3n^4sw^2}}\right), \tag{24}$$

which simplifies to

$$UA(Q) = N\sqrt{\frac{D^*\sqrt{1-\frac{4\left(\frac{nQ}{\sqrt{sw}}\right)^{6/5}}{D^{*2}}}\left(\frac{nQ}{\sqrt{sw}}\right)^{12/5}}{4g^3n^6}}, \tag{25}$$

because $\Theta(x) = 1$ for $x \geq 0$. Here the Heaviside function specifies that all stones contribute to the total wake area for the range of flow rates up to Q_D, which submerges all stones.

Example 2: Stones with a uniform distribution of diameters. This distribution corresponds to imposing a rectangular function (Figure 4a) to represent stone size over a range of diameters ($D_1 \leq D \leq D_2$), or

$$p_s(D) = \begin{cases} \frac{1}{D_2 - D_1} & D_1 \leq D \leq D_2, \\ 0 & \text{otherwise.} \end{cases} \tag{26}$$

The resulting conditional distribution of the wakes given Q is

$$p_w(A_w|Q) = \begin{cases} \frac{1}{D_2 - D_1} \frac{16A_w^3 g^6 n^6 s^3 \left(\frac{nQ}{\sqrt{s}w}\right)^{6/5} w^6}{Q^{7/2} B^2 \sqrt{\frac{\left(\frac{nQ}{\sqrt{s}w}\right)^{6/5} (4A_w^4 g^6 n^6 s^3 w^6 + Q^6 B^4)}{Q}}} & A_{w1}(Q) \le A_w \le A_{w2}(Q), \\ 0 & \text{otherwise}, \end{cases} \tag{27}$$

where $A_{w1}(Q)$ and $A_{w2}(Q)$ are given by equations (15) and (16), respectively.

The total wake area can be obtained by computing the integral equation (17) for various flow rates. This integral cannot be solved analytically and must be computed numerically. Obviously, in the limit where $D_1 \to D_2$, the area of the wake coincides with that for which all of the stones have equal diameter (i.e., the first example case).

Example 3: Stones with a truncated exponential distribution of diameters. In this case, we implement an exponential function (Figure 4a) to represent the stone size distribution as follows:

$$p_s(D) = \frac{1}{\mu_D} e^{-\frac{1}{\mu_D} D}, \tag{28}$$

where μ_D is the mean diameter of the distribution. To satisfy $\int_{D_1}^{D_2} p_s(\delta)\mathrm{d}\delta = 1$, the exponential distribution is truncated between D_1 and D_2 as

$$p_{s,\text{truncated}}(D) = \frac{p_s(D)}{P_s(D_2) - P_s(D_1)}, \tag{29}$$

where $P_s(D)$ is the cumulative distribution function of the exponential distribution. Since the concept of the derivation of the wake areas has been shown in the previous examples and also because the equations for the wakes area corresponding to the truncated exponential distribution are prohibitively long, we do not print them herein. However, they can be obtained from the data repository address (see Acknowledgments).

Example 4: Stones with a truncated gamma distribution of diameters. This example investigates the use of a gamma function (Figure 4a) to represent the size distribution of stones in terms of their diameters:

$$p_s(D) = \frac{\beta^\alpha D^{\alpha-1} e^{-\beta D}}{\Gamma(\alpha)}, \tag{30}$$

where α and β are the shape parameter and rate parameter, respectively, and $\Gamma(\alpha)$ is a complete gamma function. Similar to the exponential distribution, the gamma distribution is also truncated between D_1 and D_2 using the same procedure described above. Again, the equations for the wakes area corresponding to the truncated gamma distribution are prohibitively long, and can be accessed from the data repository address (see Acknowledgments).

3.1.2. Wake Area Distributions

Figure 4b shows the conditional distributions of the wake areas given the flow rate, Q, for the various stone size distributions presented as examples and shown in Figure 4a. As mentioned in section 2, knowing the statistical distribution of stone diameters allows for the probability density function of the wake areas to be found by using the derived distribution approach equation (13). Notice from equation (13) that as the flow rate initially increases, the probability density function $p_w(A_w, Q)$ has an area of 1 because all stones contribute to the total wake area, that is, none of them are submerged. Once the flow rate reaches the minimum Q_D for the smallest stone diameter, $p_w(A_w, Q)$ starts decreasing with flow rate and has an area less than 1 because submerged stones do not contribute to the total wake area. This generates an atom of finite probability that submerged stones no longer contribute to the total wake area. The area becomes 0 when all stones are submerged where an atom of finite probability is equal to 1.

Using equation (3), in case of $Q = 0.5\,[\frac{m^3}{s}]$, the diameter for which stones start to contribute to the wake area is $D \ge 0.33$ [m]. Except in the case of delta distribution, the size distributions used as examples included stone diameters between 0.1 to 0.7 [m]. Hence, there is a fraction of stones that are submerged and therefore not ecologically relevant in these examples. In Figure 4b, the fraction of submerged stones for uniform, truncated exponential and truncated gamma distributions is $p_w^{at}(0) = 0.39$, 0.59, and 0.19, respectively. It is worth mentioning that this result is consistent with equations (13) and (14). Since the truncated exponential distribution has a higher frequency of stones with relatively small diameters, a higher fraction of stones becomes

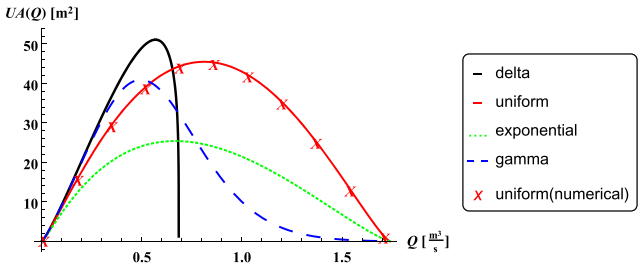

Figure 5. Total UA as a function of flow rate for the different distributions of stone sizes. UA = usable area.

submerged as the discharge increases. Conversely, based on equation (14), $\frac{dD}{dA_w}$ monotonically increases with A_w. Therefore, a size distribution of stones with a higher frequency of large diameters results in a higher frequency of large wake areas, as shown in Figure 4b. In other words, larger stones generate a more substantial contribution to the total wake areas in streams than smaller stones, as expected.

3.1.3. Total Usable Area

Figure 5 shows the total usable area resulting from the wakes that form downstream of the stones as a function of stream discharge for the example cases of stone size distributions. The highest usable area for most flow rates, especially for high flow rates, corresponds to the case with the uniform distribution of stones diameters. This is due to the fact that the uniform distribution has the highest frequency of large stones and hence, the most significant contribution to shelter zones generated by macroroughness elements. In addition, to validate the solution described in this study (section 2), the total usable area for the uniform distribution of stones diameters was also calculated numerically (i.e., red crosses in Figure 5). The numerical calculations were done by considering a discretized size distribution of macroroughnesses, $p_s(D)$, and building the UA curve by use of equations (9), (13), and (17). As shown in this figure, the proposed solution and numerically calculated total usable areas completely overlap. However, the developed solution in this study requires substantially less computational resources and therefore is more preferable.

The usable area curves shown in Figure 5 can be used to determine the environmental thresholds for the stream from equation (19). Among the four examples for stone size distributions that we consider here, the uniform distribution and truncated gamma distribution have the highest and lowest environmental thresholds, respectively. In addition to defining the environmental threshold, these curves can be used to evaluate the extent of environmental suitability for flow release policies in hydropower facilities based on the continuous magnitude under threshold (CMUT) method described in Niayifar and Perona (2017). The CMUT method calculates the magnitude of the stress period (e.g., for fishes), considering consecutive days below Q_t, by summing the difference between values of UA for the $Q < Q_t$ threshold and UA for Q_t. Then the ecological indicator is calculated as the fraction of the maximum magnitude of the stress period between regulated and nonregulated flow (see equation (8) in Niayifar and Perona, 2017).

3.2. The Impact of Stone Diameters on Threshold Flow Caused by Sediment Sorting

3.2.1. Delta Distribution

In equation (19), the environmental threshold is defined as the flow rate for which the derivative of the usable area curve becomes 0. For the delta distribution of stone diameters, this environmental threshold can be found analytically to be

$$Q_t = \frac{s^{\frac{1}{2}} w D^{\frac{1}{3}}}{n}. \tag{31}$$

Equation (31) suggests that the environmental threshold for the delta distribution scales linearly with the stream width, w. This is consistent with the fact that two identical streams that differ only by having unequal widths are expected to have environmental flow rates that are linearly proportional to their respective widths. This result also shows that a steeper slope or larger stone diameters imply a higher environmental threshold. Additionally, if the riverbed has higher roughness, n, the environmental threshold decreases. From a practical point of view, equation (31), considering unidiameter stones, can provide a very simple and robust estimation of the environmental threshold for riverine ecosystems. This simple equation only requires four parameters (i.e., s, w, D, and n) to determine the environmental threshold in a stream, which can be easily found by performing simple field surveys.

3.2.2. Gamma Distribution

In alpine streams, the stones size distribution may change temporally and spatially. The latter can happen due to changes in the stream morphology caused by climate change (e.g., Mao et al., 2017; Marchese et al., 2017) or anthropic pressure (e.g., Fan & Morris, 1992; Heinemarm, 1981; Yang et al., 2006). For example, the macroroughness element sizes in alpine streams gradually decrease from upstream to downstream due to the available mechanical energy in a stream and the associated sediment transport. To investigate this situation

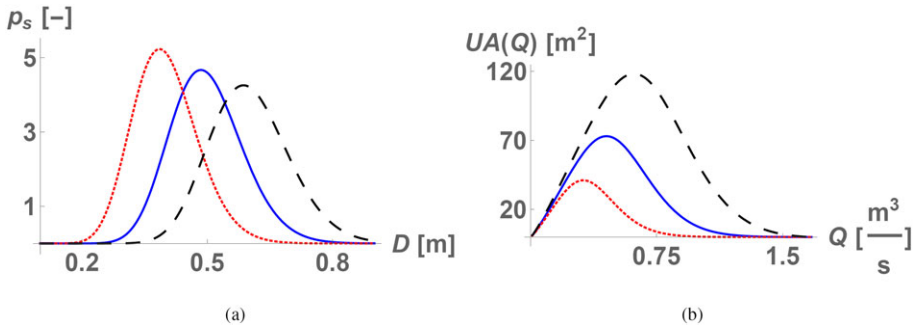

Figure 6. The impact of sediment size distribution on the usable area curve: (a) stone diameter distributions; (b) UA for different distributions of stone sizes. Dotted red, blue, and dashed black curves denote the gamma distribution with the mean of 0.4, 0.5, and 0.6 m, respectively. UA = usable area.

and its impact on the threshold flow, three gamma distributions with different mean stone diameter values (i.e., 0.4, 0.5, and 0.6 m) are considered (Figure 6a). The distributions with the highest and lowest means could mimic a spatial or temporal change in the stones size distribution. Figure 6b shows the total usable areas calculated for these different stone size distributions as a function of flow rate. From this figure, it is clear that the distributions with the smaller mean diameters result in a significant and nonlinear, decrease in the usable area generated by stones. This occurs mainly because of the loss of large stones, which generate larger contributions to the total wake area. This nonlinear relationship can strongly affect the riverine ecosystem, for example, by reducing the regions that are ecologically suitable for the fish. Furthermore, not only does this shift in size distribution generate a substantial loss in the usable area, the environmental threshold also decreases since the peak of the usable area moves toward lower discharges.

3.3. Application to Reservoir Optimal Flow Release Policies

In this section, we investigate an application of the modeled usable area generated by wakes downstream of stones and its use as ecological indicator in a multiobjective reservoir optimization case study. The new indicator is used in the direct policy search model, which was recently proposed by Niayifar and Perona (2017) to optimize the global efficiency of reservoirs. The direct policy search model uses a dynamic flow release approach to partition the flow for environmental use and energy production. The energy production is computed from the technical data (e.g., turbine characteristics and reservoir head), and the environmental efficiency associated with the flow release policies is calculated by geometrically averaging the indicators of hydrologic alteration (Richter et al., 1996) with the WUA for fishes (e.g., Niayifar & Perona, 2017; Razurel et al., 2018). Additionally, we apply the Borg MOEA (Hadka & Reed, 2013), an efficient multiobjective evolutionary algorithm, to find the optimal flow release policies (i.e., Pareto's frontier). In the case of the multiobjective reservoir optimization, Pareto's frontier consists of a set of nondominated optimal solutions if no objective (e.g., environmental indicator) can be improved without worsening at least one other objective (e.g., energy produced). Nondominated policies denote the solutions in which there is no other solution that has better quality with respect to all objectives. The reader is referred to Niayifar and Perona (2017) for details about the numerical implementation of the flow redistribution policies.

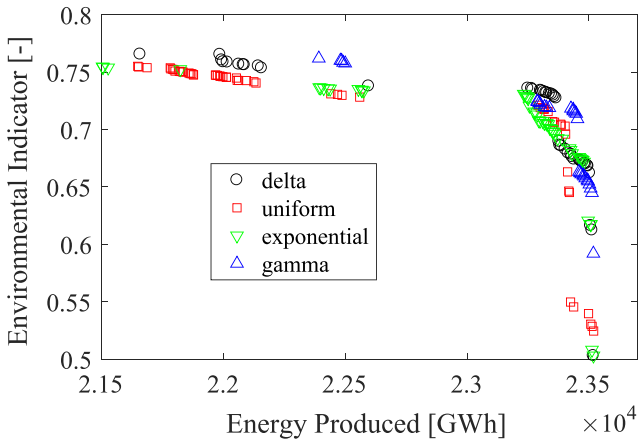

Figure 7. Pareto's frontiers simulated for different distributions of stone diameters.

The analytical model proposed in this study to calculate the usable area curve can be used to characterize the available ecological habitat generated by flow release policies in relation to the stone size distribution within the impounded river reach. To test this concept, the usable area curves in Figure 5 are used to calculate the fish indicator based on CMUT method and to develop the efficiency plot for the case study described in Niayifar and Perona (2017). Figure 7 shows the Pareto's frontiers calculated for different size distributions of stone diameters (see section 3) in the streamflow. As expected, the Pareto's frontiers corresponding to the cases with the uniform and truncated exponential distribution of stone diameters are inferior to cases with the delta and truncated gamma distributions because the latter two example cases have lower environmental thresholds. In other words, since the uniform and truncated exponential

distribution have higher frequencies of larger stones, they will have higher environmental thresholds meaning that less water from the river reach can be withdrawn for energy production. This can be seen in the Pareto's frontier by comparing equal environmental indicators for the various diameter size distributions (see Figure 7). The flow release policies near the top right of the Pareto's frontier are more ecologically and economically advantageous because they provide higher energy production without a large reduction in environmental efficiency. Therefore, the cases with delta and truncated gamma distributions have the potential to provide better global efficiencies.

4. Discussion

4.1. General Utility of the Model

Changes in natural flow regimes resulting from the ever-increasing exploitation of freshwater streams for anthropic activities (e.g., hydropower, irrigation, and urban and industrial uses) have created a critical need to develop strategies to preserve or restore riverine ecosystems. Furthermore, this need will likely be exacerbated by factors associated with climate change. The methodology developed in this work helps to characterize the environmental impacts associated with changing a stream's natural flow regime and is of vital importance for promoting more ecologically sustainable riverine ecosystem management policies.

Compared to the standard methods of calculating the WUA (e.g., from habitat modeling software packages like CASiMir and PHABSIM), the methodology proposed in this study provides a simpler technique to directly take the presence of macroroughness elements and their effects on the stream hydrodynamics into account. Owing to coarse resolution, typical habitat modeling software packages cannot capture the role that stones play in generating shelter zones for fishes or the related ecological threshold that are key to defining environmental flow release constraints (e.g., the minimum flow requirements). Our physically based, analytical model allows for calculating the usable area from quantities that can be obtained by aerial surveys (e.g., the distribution of stone diameters, channel width, slope, and Manning's coefficient of the stream). This usable area can then be used to refine WUA curves calculated from standard techniques.

To exemplify and validate the importance of the concept above, we considered four distributions of stone diameter sizes in a stream and calculated and compared their associated usable area curves. We found that the total wake area is highly sensitive to the stone diameter distributions and proved that different stone size distributions within the river reach will affect optimal water exploitation rules under various release scenarios. In the case of considering stones with the same diameter (i.e., the delta distribution), an analytical equation that only requires four parameters (i.e., s, w, D, and n) was derived to estimate the environmental threshold for the stream discharge (equation (31)). We also investigated the effect of potential temporal and spatial changes in stone size distributions in alpine streams and found that the loss of large stones significantly decreases the usable area in the stream.

The potential for our modeling tool to define sustainable environmental flow policies is thus very broad. Consider the case of hydropower, which accounts for more than 16% of the electricity generation worldwide, making fresh water the most widely used resource for renewable energy (International Energy Agency, 2015). Given its substantial footprint in the renewable energy market, hydropower operation policies must implement procedures to minimize the environmental degradation in riverine stretches downstream of dams and intakes. Hence, this study complements several recent studies that have addressed the issue above by solving multiobjective optimization problems to find the best operating policies for hydropower units (e.g., Gorla & Perona, 2013; Niayifar & Perona, 2017; Salazar et al., 2016). In general, these operation policies, which set water release rules, seek to optimize the operational efficiency of hydropower facilities with respect to multiple objectives (e.g., power production and environmental sustainability). As a demonstration, we applied the new indicator, and the usable areas calculated from our analytical solutions, to a multiobjective reservoir optimization problem and investigated shape changes of the Pareto's frontier for the different distributions of stone diameters (Figure 4). Pareto's frontier shape was found to be sensitive to stone size distributions, and of the four cases that we studied, the streams with the delta and truncated gamma distributions showed better global efficiencies compared to uniform and truncated exponential distributions.

These results suggest that the optimal minimum flow may not just change in space (i.e., the same minimum flow may be better or worse as macroroughness elements change in size from upstream to downstream) but also in time as a stream's geomorphology shifts. This is likely to be crucial from a practical point of view, especially for hydroelectric power operators and decision makers building hydropower units. For example,

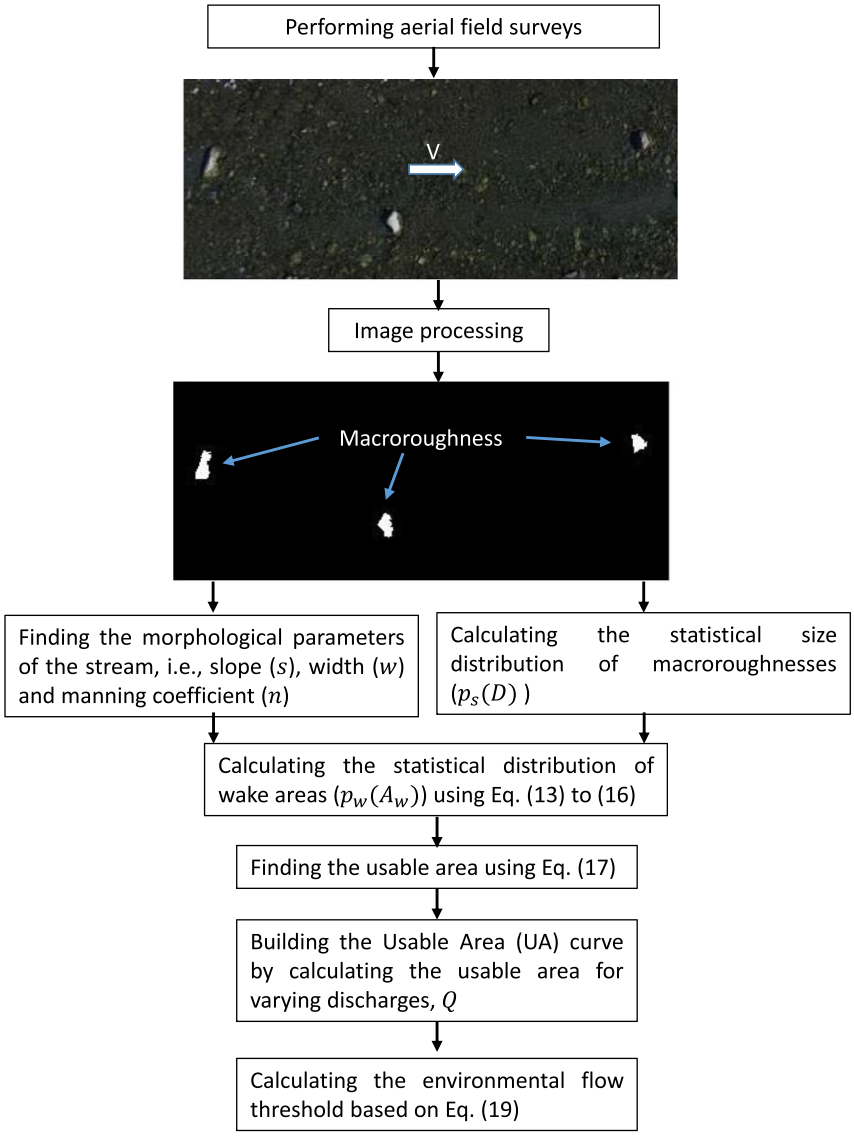

Figure 8. Overview of the model application methodology.

the methodology proposed here can be useful to better select the location of hydropower systems where maximal power production is achievable, while also considering the ecological needs.

4.2. Model Application Overview

Figure 8 shows the field survey and calculations required to characterize the ecological benefits associated with the macroroughnesses. The statistical size distribution of macroroughnesses can be obtained by taking aerial photographs with drones during the period of low stream discharge (e.g., October in the northern hemisphere). Figure 8 shows an exemplary photograph of stones distributed in a stream. Notice that this size distribution corresponds to the free surface stones diameter, *d*, and has to be converted to size of stones diameter at the stream bed, *D*, using equation (3). Stream width, *w*, can be found from the aerial images. Slope, *s*, is found by calculating the relative change in elevation with respect to the distance along the stream. Sodium chloride slug releases or other stream gauging techniques can be used to determine the stream discharge, *Q*, and velocity, *V*. Thus, the water depth can be calculated from the continuity equation for the incompressible flow ($h = \frac{Q}{Vw}$). Finally, the Manning coefficient, *n*, can be found using equation (1). Furthermore, the calculations required to calculate the usable area and the consequent environmental flow threshold have been summarized in the flowchart (Figure 8).

The usable area calculated by equation (17) considers the contribution of the wakes generated by the presence of macroroughnesses, for example, stones. While the suitable condition can vary depending on species and hydraulic conditions in the wake, we herein consider the total wake areas as the suitable habitat conditions where lower velocities have been found to be generally more favorable for species (e.g., Buffington et al., 2004; Kucukali & Cokgor, 2008). However, in the case of low flows, some areas external to the wakes (e.g., pools) may become important. Since the aerial survey will be performed in low flow periods, the base flow usable area due, for instance, to the presence of pools can be corrected by detecting the suitable areas external to the wakes from the drone images and obtain how it changes with flow by means of standard numerical simulations. It should be noted that these areas quickly will disappear as the flow rate increases. Another potential issue with this method arises when the wakes interact with each other (i.e., violating the sparse distribution assumption). In many cases for which stones are located very close to each other, they can be merged into a single stone for the sake of the habitat analyses. In a more sophisticated approach, the overlapping wake areas can be detected by geometrically sketching the boundaries of the wakes to correct the total usable area by obtaining the arrangements (i.e., positions) of stones via drone photographs. While the importance of the suitable habitat area external to the wakes during low flows and also that of the interacting wakes is case specific, we believe that they are generally negligible, and ignoring them does not cause a significant error compared to the total wake area.

The aim of this study is to present a generalized statistical approach that can be applied to efficiently investigate the ecohydraulic benefits provided by macroroughness elements, as opposed to presenting a detailed analysis for any particular stream. When it is needed, our model can easily be adapted for more case-specific studies in future works. Such studies may consider using 2-D numerical modeling in combination with the framework we present herein to obtain estimates of the wake size distributions as well as the possible suitable area external to the wakes in periods of low flows for a particular stream.

5. Conclusions

In this study, we employed the analytical model by (Negretti et al., 2006) to estimate the characteristic length scales of the wakes downstream of macroroughness elements in open channel flows and extended it to calculate the total wake area associated with various stone size distributions that generate usable habitat for fishes. The distributions of wake areas for different case studies were found by using the derived distribution approach. Subsequently, each usable area curve was built by calculating the total wake area a function of the stream discharge, and the environmental threshold was defined as the discharge for which the derivative of usable area curve becomes 0.

The methodology proposed here can be an efficient tool to calculate the environmental impacts of flow release policies. Different from common approaches to define environmental flow threshold that are solely based on hydrology (i.e., the hydrograph), our results suggests some important general principles regarding the fact that the characteristics of the stream bed, in this case, stones acting as macroroughness elements, will largely affect the optimal minimum flow release by lowering constraints to dynamic environmental flow policies. Compared to other habitat modeling approaches, which require substantial field work and do not account for the wakes downstream of macroroughness elements, the new model can be a viable alternative. Therefore, it can reduce subjectivity in interpreting streamflow requirements and developing hydropower operation policies by considering more fully the macroscale physical dynamics in streams with respect to the ecological needs for the riverine ecosystem.

Acknowledgments
We thank the Swiss National Science Foundation for funding the projects NFP70 HydroEnv (Grant 407040153942/1) and REMEDY (Grant PP00P2153028/1). The SCCER-SoE is also acknowledged for financially supporting one of the authors (H. J. O.). We acknowledge the three anonymous reviewers for their valuable suggestions, which have contributed to improving the paper. We thank members of the SBER laboratory and Hugo N. Ulloa for discussion and advice. The data used in this study are available from public repositories at https://drive.google.com/open?id=18CXUbFQI6hsPohqF6yCVHgzPZIKle253.

References

Annear, T. C., & Conder, A. L. (1984). Relative bias of several fisheries instream flow methods. *North American Journal of Fisheries Management*, *4*(4B), 531–539.

Arthington, A. H., Bunn, S. E., Poff, N. L., & Naiman, R. J. (2006). The challenge of providing environmental flow rules to sustain river ecosystems. *Ecological Applications*, *16*(4), 1311–1318.

Assani, A. A., Quessy, J.-F., Mesfioui, M., & Matteau, M. (2010). An example of application: The ecological "natural flow regime" paradigm in hydroclimatology. *Advances in Water Resources*, *33*(5), 537–545.

Biggs, B. J., Duncan, M. J., Francoeur, S. N., & Meyer, W. D. (1997). Physical characterisation of microform bed cluster refugia in 12 headwater streams, New Zealand. *New Zealand Journal of Marine and Freshwater Research*, *31*(4), 413–422.

Birsan, M.-V., Molnar, P., Burlando, P., & Pfaundler, M. (2005). Streamflow trends in Switzerland. *Journal of Hydrology*, *314*(1), 312–329.

Bloesch, J., Schneide, M., & Ortlepp, J. (2005). An application of physical habitat modelling to quantify ecological flow for the Rheinau hydropower plant, River Rhine. *Archiv für Hydrobiologie Supplementband. Large rivers*, *16*(1-2), 305–328.

Buffington, J. M., Montgomery, D. R., & Greenberg, H. M. (2004). Basin-scale availability of salmonid spawning gravel as influenced by channel type and hydraulic roughness in mountain catchments. *Canadian Journal of Fisheries and Aquatic Sciences*, *61*(11), 2085–2096.
Capra, H., Breil, P., & Souchon, Y. (1995). A new tool to interpret magnitude and duration of fish habitat variations. *Regulated Rivers: Research & Management*, *10*(2-4), 281–289.
Carolli, M., Geneletti, D., & Zolezzi, G. (2017). Assessing the impacts of water abstractions on river ecosystem services: An eco-hydraulic modelling approach. *Environmental Impact Assessment Review*, *63*(Supplement C), 136–146. https://doi.org/10.1016/j.eiar.2016.12.005
Coutanceau, M., & Bouard, R. (1977). Experimental determination of the main features of the viscous flow in the wake of a circular cylinder in uniform translation. Part 1. Steady flow. *Journal of Fluid Mechanics*, *79*(02), 231–256.
Enders, E., & Boisclair, D. (2016). Effects of environmental fluctuations on fish metabolism: Atlantic salmon salmo salar as a case study. *Journal of Fish Biology*, *88*(1), 344–358.
Enders, E. C., Boisclair, D., & Roy, A. G. (2005). A model of total swimming costs in turbulent flow for juvenile Atlantic salmon (salmo salar). *Canadian Journal of Fisheries and Aquatic Sciences*, *62*(5), 1079–1089.
Ernst, J., Dewals, B. J., Detrembleur, S., Archambeau, P., Erpicum, S., & Pirotton, M. (2010). Micro-scale flood risk analysis based on detailed 2D hydraulic modelling and high resolution geographic data. *Natural Hazards*, *55*(2), 181–209.
Fan, J., & Morris, G. L. (1992). Reservoir sedimentation. I: Delta and density current deposits. *Journal of Hydraulic Engineering*, *118*(3), 354–369.
Gippel, C. J., & Stewardson, M. J. (1998). Use of wetted perimeter in defining minimum environmental flows. *Regulated Rivers: Research & Management*, *14*(1), 53–67.
Gorla, L., & Perona, P. (2013). On quantifying ecologically sustainable flow releases in a diverted river reach. *Journal of Hydrology*, *489*, 98–107.
Hadka, D., & Reed, P. (2013). Borg: An auto-adaptive many-objective evolutionary computing framework. *Evolutionary Computation*, *21*(2), 231–259.
Hayes, J., & Jowett, I. (1994). Microhabitat models of large drift-feeding brown trout in three New Zealand rivers. *North American Journal of Fisheries Management*, *14*(4), 710–725.
Heinemarm, H. (1981). A new sediment trap efficiency curve for small reservoirs. *JAWRA Journal of the American Water Resources Association*, *17*(5), 825–830.
International Energy Agency (2015). Energy and climate change.
Kramer, D. L. (1987). Dissolved oxygen and fish behavior. *Environmental Biology of Fishes*, *18*(2), 81–92.
Kucukali, S., & Cokgor, S. (2008). Boulder-flow interaction associated with self-aeration process. *Journal of Hydraulic Research*, *46*(3), 415–419.
Lacey, R. J., Neary, V. S., Liao, J. C., Enders, E. C., & Tritico, H. M. (2012). The ipos framework: Linking fish swimming performance in altered flows from laboratory experiments to rivers. *River Research and Applications*, *28*(4), 429–443.
Lane, S., Mould, D., Carbonneau, P., Hardy, R., & Bergeron, N. (2006). Fuzzy modelling of habitat suitability using 2D and 3D hydrodynamic models: Biological challenges., Taylor & Francis.
Maddock, I. (1999). The importance of physical habitat assessment for evaluating river health. *Freshwater Biology*, *41*(2), 373–391.
Mao, L., Dell'Agnese, A., & Comiti, F. (2017). Sediment motion and velocity in a glacier-fed stream. *Geomorphology*, *291*, 69–79.
Marchese, E., Scorpio, V., Fuller, I., McColl, S., & Comiti, F. (2017). Morphological changes in Alpine rivers following the end of the Little Ice Age. *Geomorphology*, *295*(Supplement C), 811–826. https://doi.org/10.1016/j.geomorph.2017.07.018
Milhous, R. T., Updike, M. A., & Schneider, D. M. (1989). Physical habitat simulation system reference manual: Version II Tech. Rep., vol. 89, 403 pp.). Washington, DC: U.S. Fish and Wildlife Service.
Moghadam, M. K., & Keshavarzi, A. (2007). Flow separation behind habitat structure in gravel bed rivers. *Journal of Fisheries and Aquatic Science*, *2*(4), 294–301.
Moog, D. B., & Jirka, G. H. (1999). Stream reaeration in nonuniform flow: Macroroughness enhancement. *Journal of Hydraulic Engineering*, *125*(1), 11–16.
Negretti, M., Vignoli, G., Tubino, M., & Brocchini, M. (2006). On shallow-water wakes: An analytical study. *Journal of Fluid Mechanics*, *567*, 457–475.
Niayifar, A., & Perona, P. (2017). Dynamic water allocation policies improve the global efficiency of storage systems. *Advances in Water Resources*, *104*, 55–64.
Parasiewicz, P. (2007). Developing a reference habitat template and ecological management scenarios using the MesoHABSIM model. *River Research and Application*, *23*(8), 924–932.
Pasternack, G. B., Bounrisavong, M. K., & Parikh, K. K. (2008). Backwater control on riffle–pool hydraulics, fish habitat quality, and sediment transport regime in gravel-bed rivers. *Journal of Hydrology*, *357*(1-2), 125–139.
Poff, N. L., Allan, J. D., Bain, M. B., Karr, J. R., Prestegaard, K. L., Richter, B. D., et al. (1997). The natural flow regime. *BioScience*, *47*(11), 769–784.
Razurel, P., Gorla, L., Crouzy, B., & Perona, P. (2016). Non-proportional repartition rules optimize environmental flows and energy production. *Water Resources Management*, *30*(1), 207–223.
Razurel, P., Gorla, L., Tron, S., Niayifar, A., Crouzy, B., & Perona, P. (2018). Improving the ecohydrological and economic efficiency of small hydropower plants with water diversion. *Advances in Water Resources*, *113*, 249–259.
Richter, B. D., Baumgartner, J. V., Powell, J., & Braun, D. P. (1996). A method for assessing hydrologic alteration within ecosystems. *Conservation Biology*, *10*(4), 1163–1174.
Roulund, A., Sumer, B. M., Fredsøe, J., & Michelsen, J. (2005). Numerical and experimental investigation of flow and scour around a circular pile. *Journal of Fluid Mechanics*, *534*, 351–401.
Salazar, J. Z., Reed, P. M., Herman, J. D., Giuliani, M., & Castelletti, A. (2016). A diagnostic assessment of evolutionary algorithms for multi-objective surface water reservoir control. *Advances in Water Resources*, *92*, 172–185.
Schneider, M. (2001). Habitat-und Abflussmodellierung für Fließgewässer mit unscharfen Berechnungsansätzen, Inst. für Wasserbau.
Shen, Y., & Diplas, P. (2008). Application of two-and three-dimensional computational fluid dynamics models to complex ecological stream flows. *Journal of Hydrology*, *348*(1), 195–214.
Stalnaker, C., & Arnette, J. (1976). Methodologies for determining instream flows for fish and other aquatic life. Methodologies for the determination of stream resource flow requirements (Report FWS/OBS-76-03). Washington, DC: US Fish and Wildlife Service.
Taguchi, M., & Liao, J. C. (2011). Rainbow trout consume less oxygen in turbulence: The energetics of swimming behaviors at different speeds. *Journal of Experimental Biology*, *214*(9), 1428–1436.
Tennekes, H., & Lumley, J. L. (1972). *A first course in turbulence*. Cambridge: MIT Press.
Tritico, H. M., & Cotel, A. J. (2010). The effects of turbulent eddies on the stability and critical swimming speed of creek chub (Semotilus atromaculatus). *Journal of Experimental Biology*, *213*(13), 2284–2293.

Vezza, P., Parasiewicz, P., Spairani, M., & Comoglio, C. (2014). Habitat modeling in high-gradient streams: The mesoscale approach and application. *Ecological Applications*, *24*(4), 844–861.

Wilkes, M. A., Enders, E., Silva, A. T., Acreman, M., & Maddock, I. (2017). Position choice and swimming costs of juvenile Atlantic salmon salmo salar in turbulent flow. *Journal of Ecohydraulics*, *2*(1), 16–27.

Yang, Z.-S., Wang, H.-J., Saito, Y., Milliman, J., Xu, K., Qiao, S., & Shi, G. (2006). Dam impacts on the Changjiang (Yangtze) River sediment discharge to the sea: The past 55 years and after the Three Gorges Dam. *Water Resources Research*, *42*, W04407. https://doi.org/10.1029/2005WR003970